

## **ROLLING OF ROTATIONALLY SHAPED SURFACES WITH TANGENTIAL FEEDING OF THE BLANKS. FORCE CHARACTERISTICS**

*Veliko Ivanov, Aleksandar Ivanov, University of Rousse, Rousse, Bulgaria*

### **ABSTRACT**

*In this paper the dependence equations for determining the force characteristics of the process of rotationally shaped surface rolling have been presented. These are developed on the basis of similar equations used for determining the deformation force when a flat swage is inserted. A test stand and methods for experimental research have been presented. The adequacy of the mathematical models has been proved through experimental measuring. It has been determined that the radial rolling forces depend mostly on the value of radial penetration of the rolling instruments.*

### **1. INTRODUCTION**

The main force characteristics of the rolling of rotationally shaped surfaces are the radial force and the rolling moment of rotation. The radial force is needed for the strength sizing of the tools and the equipment used. The moment of rotation is necessary for determining the driving characteristics. Equations used for determining those forces, which appear at any moment of rolling of the rotationally shaped surfaces with tangential feeding of the blank have not been detected in the specialized writings. Comparing this process to thread rolling [1], we can assume that those forces can be determined through analytical methods, based on methods for determining the values of the tension, when a flat or bent swage is inserted [1, 4]. Below you will see an analytical method for determining the radial forces when rolling shaped surfaces through the tension appearing at the contact sections. Experiment results proving the adequacy of the analytical model are shown as well.

## 2. FORCE CHARACTERISTIC OF THE PROCESS WITH TANGENTIAL FEEDING OF THE BLANKS

The determining of the radial force of rolling through the tension at the contact sections is carried out under the following premises:

- the rollers are inserted in the blank as a flat trapezium-shaped swage with a thickness of one [2] (fig.1);

- the processed material is homogeneous and the elastic deformations appearing in the tool and in the blank, as well as the deformation wave appearing in front of the rollers, are ignored;

- the deformation state in the contact zone is plane oriented and the flow of the processed material is only radially oriented.

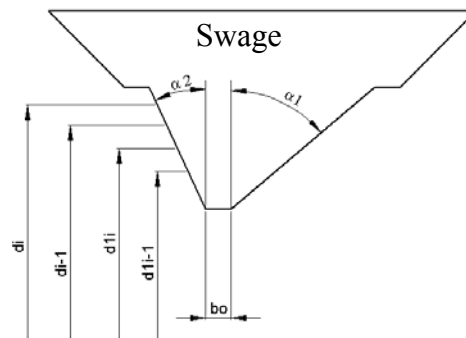


Fig.1. Current diameters at insertion of a flat swage

$d_i$ , mm – Current outer diameter of the blank rolled;  
 $d_{1i}$ , mm – Current inner diameter of the blank rolled.

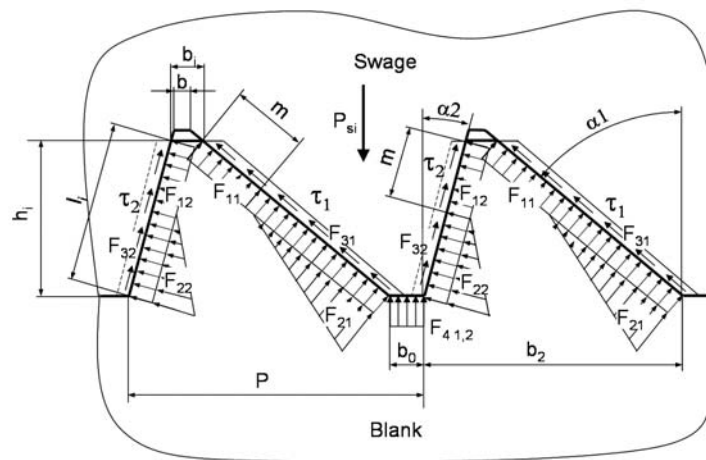


Fig.2. Tensions when inserting a flat swage

Using the symbols from fig.2 and the approach given in [1] for determining the deformation force acting  $P_{si}$  in a one pitch long section  $P$ , at any moment of the rolling process, when the molding is done along an open contour, the following equation has been worked out:

$$P_{Si} = F_{1i1} \cdot \sin \alpha_1 + F_{1i2} \cdot \sin \alpha_2 + F_{2i1} \cdot \sin \alpha_1 + F_{2i2} \cdot \sin \alpha_2 + F_{3i1} \cdot \cos \alpha_1 + F_{3i1} \cdot \cos \alpha_1 + F_{4i1} + F_{4i2} \quad (1)$$

where

$$\begin{aligned}
 F_{1i1,2} &= \frac{2}{\sqrt{3}} \cdot \sigma_i \left( 1 - \frac{\psi_y - 1}{\mu_{\max 1,2}} \right) \frac{h_i}{\cos(\alpha_{1,2})} \cdot a_i' \\
 F_{2i1,2} &= \frac{1}{\sqrt{3}} \cdot \frac{\sigma_i}{\alpha_{1,2}} \left[ b_i \cdot \ln \left( \frac{b_{i1,2}}{b_{3 1,2}} \right) - (b_{i1,2} - b_{3 1,2}) \right] \cdot a_i' \\
 F_{3i1,2} &= \frac{1}{\sqrt{3}} \cdot \sigma_i \cdot \frac{h_i}{\cos(\alpha_{1,2})} \cdot \frac{\mu}{\mu_{\max 1,2}} \cdot a_i' \\
 F_{4i1} &= \frac{1}{\sqrt{3}} \cdot \sigma_i \cdot b_{01} \cdot \left[ 1 + \pi - \alpha_1 + \frac{1}{4\alpha_1} \ln \left( \frac{P - b_0}{b_{3 1}} \right) + \left( \frac{\psi_{xi} - 1 + 0,5 \cdot \pi}{\mu_{\max 1}} \right) \cdot \mu \right] \cdot a_i' \\
 F_{4i2} &= \frac{1}{\sqrt{3}} \cdot \sigma_i \cdot (b_0 - b_{01}) \cdot \left[ 1 + \pi - \alpha_2 + \frac{1}{4\alpha_2} \ln \left( \frac{P - b_0}{b_{3 2}} \right) + \left( \frac{\psi_{xi} - 1 + 0,5 \cdot \pi}{\mu_{\max 2}} \right) \cdot \mu \right] \cdot a_i' \quad (2)
 \end{aligned}$$

$F_{1i1}, F_{1i2}, N$  – invariable constituent of the normal loading, originating at the side contact areas with profile angles  $\alpha_1$  and  $\alpha_2$ , respectively;

$F_{2i1}, F_{2i2}, N$  – invariable constituent of the normal loading, originating at the side contact areas with profile angles  $\alpha_1$  and  $\alpha_2$ , respectively;

$F_{3i1}, F_{3i2}, N$  – tangential force at the side contact areas with profile angles  $\alpha_1$  and  $\alpha_2$ , respectively;

$F_{4i1}, F_{4i2}, N$  – normal forces at the contact area  $b_0$  when rolling along an open contour with profile angles  $\alpha_1$  and  $\alpha_2$ , respectively;

$a_i'$ , mm – length of deformation zone;

$\mu$  – friction quotient;

$\mu_{1,2max}$  – maximum friction quotient along the contact surfaces.

The real tension due to deformation when rolling is effected in a non-heated state  $\sigma_i$ , used in (2), are usually determined after the equation [1]:

$$\sigma_i = \frac{R_m}{1 - \psi_y} \cdot \left( \frac{\psi_{xi}}{\psi_y} \right)^{\frac{\psi_y}{1 - \psi_y}}, \quad (3)$$

where

$$\psi_{xi} = \frac{(d_i - d_{1i} - d_{i-1} + d_{1i-1})(\cos \alpha_1 + \cos \alpha_2)}{2b_0 + (d_i - d_{1i})(\cos \alpha_1 + \cos \alpha_2)}$$

is the degree of deformation at any moment of the insertion of a swage (fig.1) with a non-symmetric shape ( $\alpha_1 \neq \alpha_2$ );

$\psi_y = 0,2 - 0,05$  -relative shrinking of the cross section at the moment of journal formation, when a model of extension destruction is tested.

For dimensions of the processed part [2], the current values of radial forces  $P_{si}$  at radial insertion  $\Delta r_i$  of the tools for  $d_0' = 100\text{mm}$  are determined by means of Excel electronic tables and the interactive medium for engineering and scientific calculation of the MATLAB system (Table 1). The graphic interpretation of the results obtained is shown on fig.3.

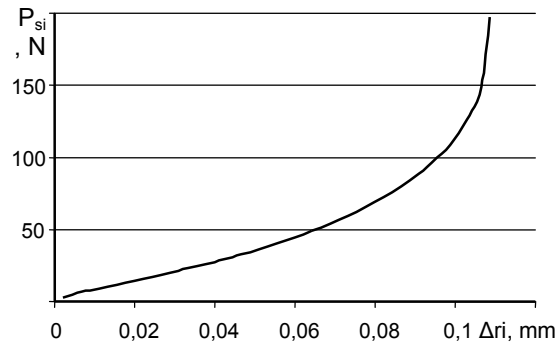


Table 1. Force load at radial insertion  $\Delta r_i$

$\Delta r_i$ , mm	$P_{si}$ , N
0,0244	21,28
0,0510	45,35
0,0754	77,97
0,1087	246,68

Fig.3. Change of force load during rolling depending on the insertion  $\Delta r_i$  of the tools with  $d_0 = 100\text{ mm}$  with  $dz = 1.4\text{mm}$ .

### 3. EXPERIMENTAL RESEARCH

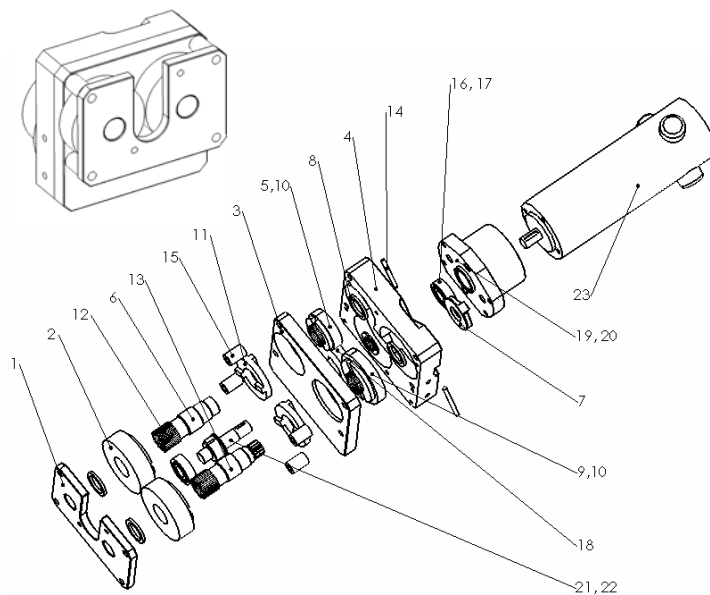


Fig.4. Axonometric model of the rolling test stand:

1 Support; 2 Rollers; 3 Cover; 4 Body; 5 Driving gear; 6 Driving shaft; 7 Regulator; 8 Washer; 9 Driven gear; 10 Needle roll bearing; 11 Joint; 12 Needle roll bearing; 13 Driven shaft; 14 Regulating screws; 15 Distance bush; 16 Bearing; 17 Seal; 18 Central gear; 19 Joint; 20 Cup; 22 Central shaft; 23 Electric motor.

### 3.1. TEST STAND

On fig.4 the principal view and the expanded axonometric model of the rolling test stand is shown. The rolling stand is driven by a direct current electrical motor – reduction gear (23), which transmits the rotation to the driving and driven rollers (2) with respective transmission ratio  $i_{r.s.}$  10/7 and 1, using a system of gears. Thus the rollers with equal diameters with bearings lying on the axes, rotate with angular speeds correlating as follows  $K=\omega_1/\omega_2=0,7$ . To provide accuracy of rolling and to regulate the distance between the axes, one of the shafts is supposed to have a cam step.

### 3.2. RESEARCH METHODS

Since the radial rolling force cannot be measured directly, it is done indirectly through the equation

$$F_{roi} = F_{toi} / K_F, [1] \quad (4)$$

where  $K_F = (0,12 - 0,18)$  – the correlation between the tangential and the radial force [1]. The tangential rolling force  $F_{toi}$  is determined after the formula

$$F_{toi} = \frac{M_{e.m.i}}{d'_{wi} \cdot i_{r.s.} \cdot i_{h.r.s.}} \quad (5)$$

where  $M_{e.m.i}$  is the motor's moment of rotation;

$i_{h.r.s.}=1/6$  – transmission ratio of the heliocentric type reducer;

$i_{r.s.}=10/7$  – transmission ratio of the rolling test stand gear;

$d'_{wi}$  – is the centroid diameter of the driving roller at radial insertion  $\Delta r_i$  of the rollers in the blank.

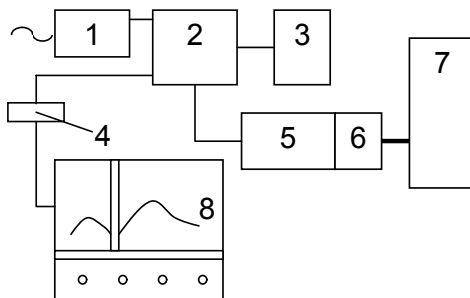


Fig.5 Diagram of the measuring test stand:

- 1-Transformer (AQ Magnit AD); 2-Direct current transistor converter (ERTAC A-10);
- 3-Control panel; 4-By-pass with coefficient  $K_{By-pass}=20A/75mV$ ;
- 5-Direct current electric motor (DC PM SERVO MOTOR);
- 6-Helocentric type reducer with transmission ratio 1/6; 7-Test roller; 8-XY recorder.

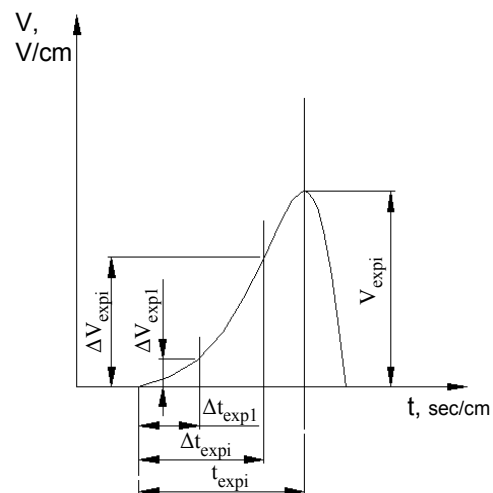


Fig.6. Data from the XY recorder

Since the straight line motor characteristic  $K_{e.m.} = 1,3/8$  Nm/A is known (rated moment of rotation 1,3Nm with consumed electricity 8A), the motor's moment of rotation  $M_{e.m.i}$  is

$$M_{e.m.i} = K_{e.m.} \cdot I_{e.m.i} , \quad (6)$$

where  $I_{e.m.i}$  is the value of motor's current, calculated using the equation

$$I_{e.m.i} = \Delta V_{exp.i} \cdot K_{By-pass} , \quad (7)$$

and  $K_{By-pass} = 20A/75mV$  is the invariable constant of the by-pass used;

$\Delta V_{exp.i}$  – by-pass tension at the  $i$ -th moment.

To measure the voltage  $\Delta V_{exp.i}$  of the by-pass, the measuring and recording configuration is worked out on fig.5.

The XY–recorder records the changing of by-pass voltage in real time  $t_{exp.i}$  of the  $i$ -th blank (fig.6). For each separate rolled blank a coefficient  $Kt_i$  is defined to measure the correlation between the theoretical process time  $\Delta t$  and the real time necessary to process the blank  $t_{exp.i}$ , defined experimentally after the formula

$$Kt_i = \Delta t / t_{exp.i} . \quad (8)$$

For each graph recorded, several values of the by-pass voltage are measured  $\Delta V_{exp.i}$  with different  $t_{exp.i}$  (fig.6). To determine the real insertion  $\Delta r_i$ , corresponding to voltages  $\Delta V_{exp.i}$ , the following equation is used

$$\Delta t_i = Kt_i \cdot \Delta t_{exp} . \quad (9)$$

where the relation  $\Delta r_i$  and  $\Delta t_i$  has been determined after equations in [3].

### 3.3. RESULTS FROM THE EXPERIMENTAL RESEARCH

For the data of the processed part [2] through the algorithm described with the equations (4) through (9), with roller diameter  $d_o = 97,7$ mm and for length of part one step of the rolled shape  $P=0,6$ mm, the maximum rolling forces  $F_{rmax}$  have been determined, for 8 different peripheral speeds of the driving roller and a tenfold repetition of experiments for each peripheral speed (Table 2, Table 3), with coefficient  $K_F=0,15$ . For the values of the maximum radial rolling force

Table 2. Maximum radial force  $F_{rmax}$ ,  
N of rolling for different peripheral speeds of the roller and  $dz=1,4$ mm and  $K_F=0,15$ .

Experiment, №	$V_0', m/min$							
	1,151	2,578	4,297	9,515	17,802	22,099	28,852	41,743
1	168,060	144,076	131,352	128,149	98,920	91,217	81,082	59,352
2	142,002	152,538	151,254	131,708	103,987	81,082	82,095	54,000
3	166,796	147,818	155,677	133,488	93,823	81,082	71,514	58,935
4	153,244	158,920	128,333	122,151	111,119	89,190	68,214	69,890
5	145,947	130,849	159,569	119,676	89,190	87,568	67,250	72,973
6	152,202	136,052	148,866	123,738	100,338	89,190	64,342	66,964
7	162,974	154,169	160,542	142,298	98,322	85,947	79,954	55,460
8	139,692	160,542	145,947	126,487	100,338	80,128	65,061	70,619
9	148,032	150,812	140,474	128,076	109,460	84,325	75,147	75,327
10	149,689	160,336	147,974	134,611	97,298	88,176	64,217	63,558
$\Sigma(F_{ri} max)/10$	152,864	149,611	146,999	129,038	100,280	85,790	71,888	64,708

Table 3. Maximum radial force  $F_{rmax}$ ,  
N of rolling for different peripheral speeds of the roller and  $dz=1,2mm$  and  $K_F=0,15$ .

Experiment, №	$V_0', m/min$							
	1,151	2,363	4,091	8,748	16,881	23,020	29,711	47,820
1	154,057	120,095	110,125	105,813	92,178	72,974	48,649	37,048
2	131,022	127,705	103,522	98,323	78,281	64,489	41,246	38,146
3	131,354	110,351	118,622	103,848	83,399	60,715	66,459	33,395
4	128,150	126,046	111,790	100,542	93,597	64,217	65,013	32,692
5	116,759	127,281	120,193	104,249	89,904	72,974	59,422	26,855
6	131,671	110,023	111,488	89,191	75,059	69,801	46,251	30,959
7	125,366	118,149	122,152	109,461	91,218	70,582	56,816	28,109
8	116,759	106,655	111,608	115,299	71,388	56,226	42,491	34,402
9	127,705	117,143	120,608	102,932	84,650	67,720	44,643	40,350
10	131,710	119,886	104,249	101,353	92,521	61,452	48,997	25,906
$\Sigma(F_{rmax})/10$	<b>129,455</b>	<b>118,333</b>	<b>113,436</b>	<b>103,101</b>	<b>85,220</b>	<b>66,115</b>	<b>51,999</b>	<b>32,786</b>

$F_{rmax}$  shown in (Table 2, Table 3), with the help of an algorithm specially worked out in MATLAB, following the method of the smallest squares, the coefficients  $a_1$ ,  $a_2$  and  $a_3$  (Table 4) of the approximating polynomial  $P_{apr}$  of second power have been determined.

$$F_{rmax apr} = a_1 \cdot V_0'^2 + a_2 \cdot V_0' + a_3 \quad (10)$$

On fig.7 is shown the graph describing the influence of rolling speed on the radial force. It can be seen that with the increase of  $V_0'$  the radial force decreases.

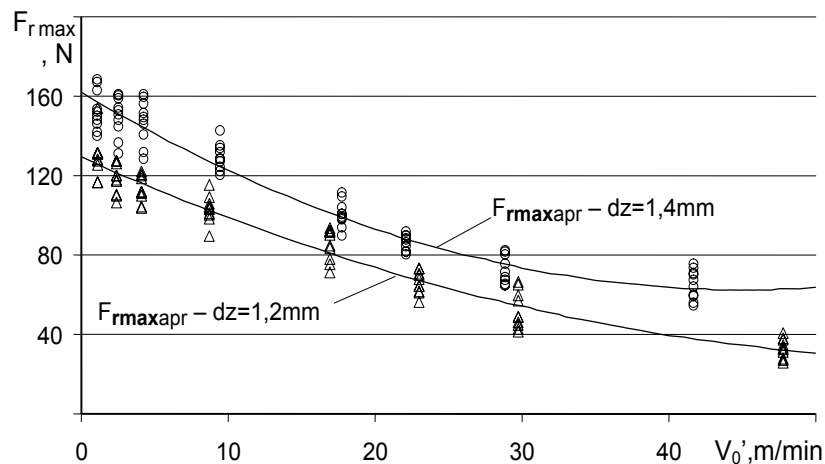


Fig.7. Change of  $F_{rmax}$  and  $F_{rmax apr}$  depending on the change of peripheral speed  $V_0'$  for  $K_F=0,15$ .

“o” and “Δ” – experimentally defined values of  $F_{rmax}$  for  $dz=1,4mm$  and  $dz=1,2mm$ .

Table 4. Coefficients of the approximating polynomial curves for different values of  $dz=1,4\text{mm}$  and  $dz=1,2\text{mm}$  for the max. radial rolling force  $F_{r\max}$  and  $K_F=0,15$ .

$P_{apr}$	$a_1$	$a_2$	$a_3$
$dz=1,2$	0,0271	-3,3305	129,403
$dz=1,4$	0,0493	-4,4286	161,983

Research has been conducted on the influence of insertion  $\Delta r_i$  with different peripheral speeds  $V_o'$ , on the changing of the radial force  $F_{ri}$ . After processing of the experimental data using the method of the smallest squares, the values of the coefficients  $b_1$ ,  $b_2$  and  $b_3$  and the approximating polynomial of second power expressing the dependence of the radial force  $F_{ri}$  on the insertion  $\Delta r_i$ , have been determined:

$$F_{ri\text{ apr}} = b_1 \Delta r_i^2 + b_2 \Delta r_i + b_3 \quad (11)$$

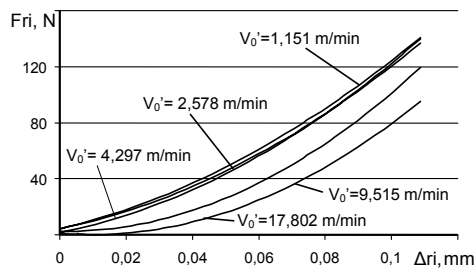


Fig.8 Change of  $F_{ri}$  for  $dz=1,4\text{mm}$ ,  $K_F=0,15$  depending on the changing of the radial insertion  $\Delta r_i$  for different peripheral speeds.

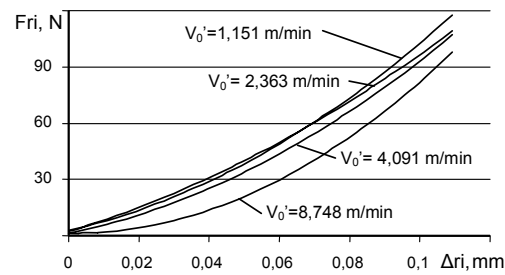


Fig.9 Change of  $F_{ri}$  for  $dz=1,2\text{mm}$ ,  $K_F=0,15$  depending on the changing of the radial insertion  $\Delta r_i$  for different peripheral speeds.

The values of these coefficients are shown in Table 5 and Table 6 for rolling of blanks with two different diameters-  $dz=1,4\text{mm}$  and  $dz=1,2\text{mm}$  for  $K_F=0,15$ . The graphs of this influence are given in fig.8 and fig 9.

Table 5 Coefficients of the approximating polynomial curves  $F_{ri\text{ apr}}$  for different values of  $V_o'$  u  $dz=1,4\text{mm}$  and  $K_F=0,15$ .

$V_o', \text{m/min}$	1,151	2,578	4,297	9,515	17,802
$b_1$	6372,841	6777,404	7428,144	10297,604	9722,038
$b_2$	565,267	481,625	463,897	-44,995	-189,519
$b_3$	4,002	4,352	1,559	2,550	1,018

Table 6. Coefficients of the approximating polynomial curves  $F_{ri\text{ apr}}$  for different values of  $V_o'$  u  $dz=1,2\text{mm}$  and  $K_F=0,15$

$V_o', \text{m/min}$	1,151	2,363	4,091	8,748
$b_1$	5731,696	3756,066	5361,438	8287,626
$b_2$	423,723	566,619	381,977	-22,798
$b_3$	2,801	2,230	1,317	1,307



Fig.10 and 11 show the graphs comparing the analytically determined values of the radial force under equation (1) and the experimentally determined under the above mentioned method approximating curves (11) for  $K_F=0,11$  and  $K_F=0,20$ . It is observed that for low speeds -  $V_0'=1,151$  m/min- there is a good coincidence of the theoretical and experimental results. An insignificant diversion is observed only at the last stage of rolling. This allows for the results achieved under the analytical model to be used further for determining the full radial load of the rollers, considering the real rolled surface of the part.

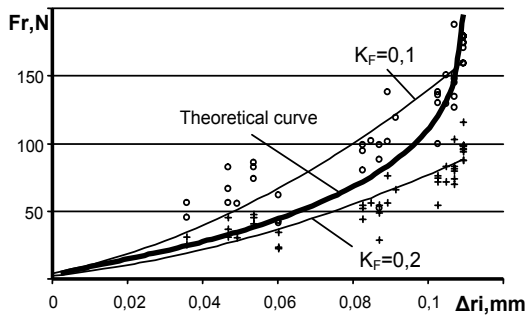


Fig.10 .  $F_{ri}$  for  $dz=1,4$ mm depending on the changing of the radial insertion and analytically defined equation for measuring the force load.

o and + : experimental values for  $F_{ri}$  for  $K_F=0,11$  and  $K_F=0,20$

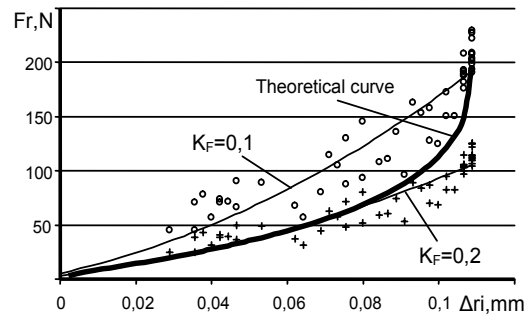


Fig.11 .  $F_{ri}$  for  $dz=1,2$ mm depending on the changing of the radial insertion and analytically defined equation for measuring the force load.

o and + : experimental values for  $F_{ri}$  for  $K_F=0,11$  and  $K_F=0,20$

#### 4. CONCLUSIONS

1. The change and the value of the force characteristics during rolling does not depend substantially on the diameter of the rollers  $d_0$  ;
2. With the increase of the peripheral speed of the rollers, the value of the maximum radial force during rolling with tangential feeding of the blanks decreases;
3. The insertion  $\Delta r_i$  of the tools into the blank influences strongly the change and the value of the force characteristics during rolling;
4. The analytical equation determining the force load during rolling adequately describes the experimentally defined load if the coefficient is within the range  $K_F=0,11-0,20$  and the rolling speed is minimal.

#### 5. REFERENCE

- [1]. V. Ivanov. *Thread-rolling tools – theory, design, implementation*. Rouse, 2000.
- [2]. V. Ivanov, Al. Ivanov. *Rolling of rotationally shaped surfaces with tangential feeding of the blanks. Kinematics and output*. Part 1
- [3]. V. Ivanov, Al. Ivanov. *Defining the speed of movement of the blank between the rollers during rolling of rotational surfaces with tangential feeding*. Proceedings, volume 39, series 7, “Machine-building sciences”, Rouse, 2002.
- [4]. G. Smirnov - Aljaev. *Material resistance during plastic deformation*. Leningrad, Machine-building, 1978.

## VALJANJE ROTACIONO PROFILISANIH POVRŠINA SA TANGENCIJALNIM DOTUROM PRIPREMKA

*Veliko Ivanov, Aleksandar Ivanov*

### REZIME

Glavne energetske karakteristike kod valjanja rotaciono profilisanih površina su radijalne sile i moment valjanja. Upoređujući navedeni proces sa valjanjem navoja, može se pretpostaviti da ti parametri mogu biti određeni analitičkim putem.

U radu se daje analitički pristup kojim je moguće odrediti radijalne sile za slučaj valjanja profilisanih površina. Pri tome se uvode određene pretpostavke koje su u radu detaljno navedene i argumentovane.

Verifikacija analitičkog metoda izvršena je eksperimentalnim istraživanjima. Za tu svrhu je konstruisano i realizovano specijalno eksperimentalno postrojenje kod koga je valjaonički uređaj pogonjen elektro-motorom (preko određenog reduktora).

Obzirom da se radijalna sila nije mogla direktno meriti, to je realizovano preko odnosa:

$$F_{roi} = F_{toi} / K_F \quad \text{gde je } K_F = (0,12 \div 0,18) - \text{korelacija između tangencijalne i radijalne sile.}$$

Pri tom je tangencijalna sila valjanja  $F_{toi}$ :

$$F_{toi} = \frac{M_{e.m.i}}{d_{wi} \cdot i_{r.s.} \cdot i_{h.r.s.}}$$

$M_{e.m.i}$  – moment el. motora;

$i_{h.r.s.} = 1/6$  – odnos hidrocentričnog prenosa;

$i_{r.s.} = 10/7$  – prenosni odnos zupčastog reduktora;

$d_{wi}$  – prečnik pogonskog valjka

Na osnovu analitičkih razmatranja i eksperimentalnih istraživanja autori donose sledeće zaključke:

1. Promena i vrednost sile za vreme valjanja ne zavisi od prečnika valjaka  $d_o$
2. Povećanjem periferne brzine valjanja maksimalna radijalna sila za vreme valjanja sa tangencijalnim doturom priprema opada
3. Analitički izrazi za određivanje sile pokazuju visok nivo slaganja sa eksperimentalno određenom silom u slučaju da je koeficijent  $K$  u opsegu  $0,11 \div 0,20$  a brzina valjanja minimalna.